Differentiated human airway organoids to assess infectivity of emerging influenza virus

Jie Zhou[a,b,c,1], Cun Li[b,1], Norman Sachs[d,1], Man Chun Chiu[b], Bosco Ho-Yin Wong[b], Hin Chu[a,b,c], Vincent Kwok-Man Poon[b], Dong Wang[b], Xiaoyu Zhao[b], Lei Wen[b], Wenjun Song[b,e], Shuofeng Yuan[b], Kenneth Kak-Yuen Wong[f], Jasper Fuk-Woo Chan[a,b,c,g,h], Kelvin Kai-Wang To[a,b,c,g,h], Honglin Chen[a,b,c], Hans Clevers[d,i,2,3], and Kwok-Yung Yuen[a,b,c,g,h,2,3]

[a]State Key Laboratory of Emerging Infectious Diseases, The University of Hong Kong, Hong Kong; [b]Department of Microbiology, The University of Hong Kong, Pokfulam, Hong Kong; [c]Research Centre of Infection and Immunology, The University of Hong Kong, Hong Kong; [d]Hubrecht Institute, Royal Netherlands Academy of Arts and Sciences, 3584 CT Utrecht, The Netherlands; [e]Institute of Integration of Traditional and Western Medicine, Guangzhou Medical University, Guangzhou 510180, China; [f]Department of Surgery, Queen Mary Hospital, Hong Kong; [g]Carol Yu Centre for Infection, The University of Hong Kong, Hong Kong; [h]The Collaborative Innovation Center for Diagnosis and Treatment of Infectious Diseases, The University of Hong Kong, Hong Kong; and [i]Princess Maxima Center for Pediatric Oncology, 3584 CT Utrecht, The Netherlands

Contributed by Hans Clevers, May 15, 2018 (sent for review April 13, 2018; reviewed by Pei-Jer Chen and Bernard Roizman)

Novel reassortant avian influenza H7N9 virus and pandemic 2009 H1N1 (H1N1pdm) virus cause human infections, while avian H7N2 and swine H1N1 virus mainly infect birds and pigs, respectively. There is no robust in vitro model for assessing the infectivity of emerging viruses in humans. Based on a recently established method, we generated long-term expanding 3D human airway organoids which accommodate four types of airway epithelial cells: ciliated, goblet, club, and basal cells. We report differentiation conditions which increase ciliated cell numbers to a nearly physiological level with synchronously beating cilia readily discernible in every organoid. In addition, the differentiation conditions induce elevated levels of serine proteases, which are essential for productive infection of human influenza viruses and low-pathogenic avian influenza viruses. We also established improved 2D monolayer culture conditions for the differentiated airway organoids. To demonstrate the ability of differentiated airway organoids to identify human-infective virus, 3D and 2D differentiated airway organoids are applied to evaluate two pairs of viruses with known distinct infectivity in humans, H7N9/Ah versus H7N2 and H1N1pdm versus an H1N1 strain isolated from swine (H1N1sw). The human-infective H7N9/Ah virus replicated more robustly than the poorly human-infective H7N2 virus; the highly human-infective H1N1pdm virus replicated to a higher titer than the counterpart H1N1sw. Collectively, we developed differentiated human airway organoids which can morphologically and functionally simulate human airway epithelium. These differentiated airway organoids can be applied for rapid assessment of the infectivity of emerging respiratory viruses to human.

airway organoid | proximal differentiation | influenza virus | infectivity

Influenza A viruses (IAVs) can infect a diversity of avian and mammalian species, including humans, and have the remarkable capacity to evolve and adapt to new hosts (1). The segmented RNA genomes of IAVs and the low fidelity of RNA polymerase allow antigenic shift and drift, which drive the viral evolution. Thus, novel viruses from birds and pigs cross the species barrier and infect humans, leading to sporadic infections, epidemics, and even pandemics (1, 2). Despite the tremendous progress made in virology and epidemiology, which subtype or strain of IAV will cause the next outbreak remains unpredictable. A novel reassortant H7N9 influenza virus from poultry has led to recurrent outbreaks of human infection in China since 2013 (2, 3). More than 1,500 laboratory-confirmed cases of H7N9 human infections were reported by October 2017, with a case-fatality rate higher than 35% (4). In 2009, the first influenza pandemic of the 21st century was caused by a novel pandemic H1N1 (H1N1pdm), which originated via multiple reassortments of "classical" swine H1N1 virus with human H3N2 virus, avian virus, and avian-like swine virus (5). While swine viruses infect humans only sporadically, this novel strain of swine-derived H1N1pdm virus has infected a large proportion of the human population, establishing sustained human-to-human transmission and circulating globally as a seasonal virus strain since then.

Proteolytic cleavage of viral glycoprotein HA is essential for IAV to acquire infectivity, since only the cleaved HA molecule mediates the membrane fusion between the virus and the host cell, a process required for the initiation of infection. HA proteins of low-pathogenic avian IAVs and human IAVs carry a single basic amino acid arginine at the cleavage site (6, 7), recognized by trypsin-like serine proteases. Productive infection of

Significance

Influenza virus infection represents a major threat to public health worldwide. There is no biologically relevant, reproducible, and readily available in vitro model for predicting the infectivity of influenza viruses in humans. Based on the long-term expanding 3D human airway organoids, we developed proximal differentiation and further established a 2D monolayer culture of airway organoids. The resultant 3D and 2D proximal differentiated airway organoids can morphologically and functionally simulate human airway epithelium and as a proof of concept can discriminate human-infective influenza viruses from poorly human-infective viruses. Thus, the proximal differentiated airway organoids can be utilized to predict the infectivity of influenza viruses and, more broadly, provide a universal platform for studying the biology and pathology of the human airway.

Author contributions: J.Z., H. Chen, H. Clevers, and K.-Y.Y. designed research; J.Z., C.L., M.C.C., B.H.-Y.W., H. Chu, V.K.-M.P., D.W., X.Z., L.W., W.S., S.Y., and K.K.-Y.W. performed research; N.S. and H. Clevers contributed new reagents/analytic tools; J.Z., C.L., M.C.C., B.H.-Y.W., H. Chu, J.F.-W.C., K.K.-W.T., H. Chen, and K.-Y.Y. analyzed data; and J.Z., H. Chen, H. Clevers, and K.-Y.Y. wrote the paper.

Reviewers: P.-J.C., Graduate Institute of Clinical Medicine; and B.R., The University of Chicago and Shenzhen International Institute for Biomedical Research.

The authors declare no conflict of interest.

Data deposition: The sequences reported in this paper have been deposited in the GenBank database [A/swine/Guangdong/07 HA (H1N1sw) accession no. MH293472 and Avian H7N2 HA (A/pigeon/Zhejiang/DTID-ZJU01/1-1/2013) accession no. MH186147].

[1]J.Z., C.L., and N.S. contributed equally to this work.

[2]H. Clevers and K.-Y.Y. contributed equally to this work.

[3]To whom correspondence may be addressed. Email: h.clevers@hubrecht.eu or kyyuen@hku.hk.

This article contains supporting information online at www.pnas.org/lookup/suppl/doi:10.1073/pnas.1806308115/-/DCSupplemental.

Published online June 11, 2018.

these viruses in the human airway thus requires serine proteases such as TMPRSS2, TMPRSS4, HAT, and others (8). However, HA proteins of highly pathogenic avian viruses, such as H5N1, contain a polybasic cleavage site which is activated by ubiquitously expressed proteases. Current in vitro models for studying influenza infection in the human respiratory tract involve short-term cultures of human lung explants and primary airway epithelial cells. Human lung explants are not readily available on a routine basis. In addition, the rapid deterioration of primary tissue is a major problem in infection experiments, since there is no protocol to maintain tissue viability in vitro. Under air–liquid interface conditions, basal cells isolated from human airway can polarize and undergo mucociliary differentiation. However, this capacity is lost within two or three passages (9). Collectively, these primary tissues and cells hardly constitute a convenient, reproducible model to study human respiratory pathogens. Although various cell lines, e.g., A549 and Madin–Darby canine kidney (MDCK) cells, have been commonly used to propagate influenza viruses and to study their virology, they poorly recapitulate the histology of human airway epithelium. In addition, due to the low serine protease activity, most cell lines do not support the growth of the influenza viruses with a monobasic HA cleavage site unless the culture medium is supplemented with an exogenous serine protease, trypsin treated with *N*-tosyl-L-phenylalanine chloromethyl ketone (TPCK). Thus, a biologically relevant, reproducible, and readily available in vitro model remains urgently needed for studying the biology and pathology of the human respiratory tract.

Recent advances in stem cell biology have allowed the in vitro growth of 3D organoids that recapitulate the essential attributes of their counterpart organs in vivo. These organoids can be grown from pluripotent stem cells (PSCs) or tissue-resident adult stem cells (ASCs) (10). ASC-derived organoids consist exclusively of epithelial cells and can be generated from a variety of human organs, the first being the human gut (11). These human intestinal organoids represent the first model for in vitro propagation of Norovirus and have allowed the study of other viruses (12, 13). We very recently described the initial conditions for expanding human ASC-derived airway organoids (AOs) for >1 y (14). Of note, protocols also have been established for generating lung organoids from human PSCs and embryonic lung (15, 16).

Results

Characterization of the Human AOs. Based on the recently reported protocol (14), we established several lines of AOs from small pieces of normal lung tissue adjacent to the diseased tissue from patients undergoing surgical resection for clinical conditions. These AOs, 3D cysts lined by polarized epithelium, accommodated the four major types of airway epithelial cells, i.e., ciliated cells (ACCTUB$^+$ or FOXJ1$^+$), goblet cells (MUC5AC$^+$), basal cells (P63$^+$), and club cells (CC10$^+$) (Fig. 1*A*). Apical ACCTUB clearly indicated the orientation of polarization. Most organoids are orientated towards the lumen (Fig. 1*A*, ACCTUB *Left*), while a small proportion of the organoids are inverted (Fig. 1*A*, ACCTUB *Right*). Beating cilia were visible (Movie S1). No type I and type II alveolar epithelial cells were present. Thus, these organoids resembled the pseudostratified ciliated airway epithelium. The AOs were inoculated with human IAV H1N1pdm, the low-pathogenic avian virus H7N9/Ah, and the highly pathogenic avian virus H5N1. The intracellular (cell lysate) viral loads of all three virus strains increased over 2 $\log_{10}$ units (Fig. 1*B*). The extracellular (supernatant) viral loads, especially the viral titers, were elevated by 2–3 $\log_{10}$ units.

Ciliary beating plays an essential role in human airway biology and pathology, and 50–80% of airway epithelial cells are ciliated (17). However, immunostaining (Fig. 1*A*) and flow cytometry indicated that ciliated cells were apparently underrepresented in these

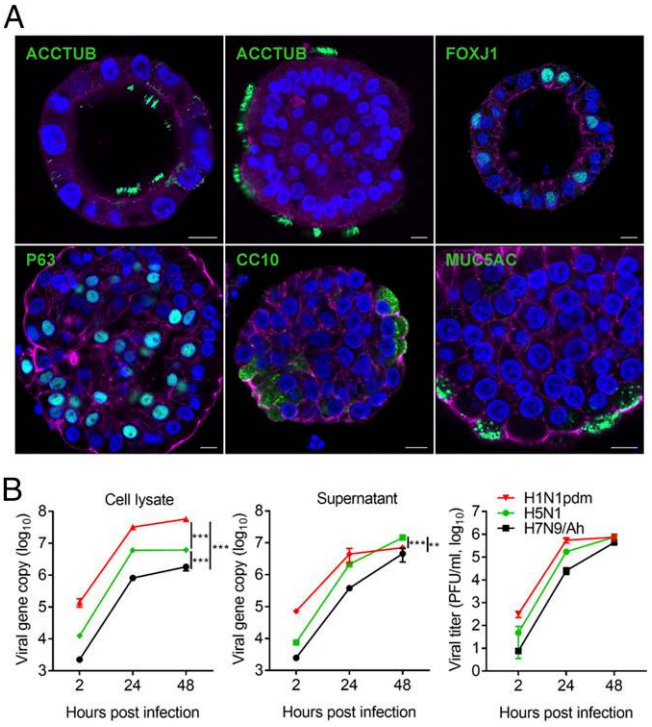

Fig. 1. Demonstration of four types of airway epithelial cells and replication of influenza viruses in human AOs. (*A*) Four lineages of airway epithelial cells are identified in the human AOs, i.e., ACCUB$^+$ and FOXJ1$^+$ ciliated cells, P63$^+$ basal cells, CC10$^+$ club cells, and MUC5AC$^+$ goblet cells. Nuclei and cellular actin filaments were counterstained with DAPI (blue) and Phalloidin-647 (purple), respectively. (Scale bars, 10 μm.) (*B*) The AOs (n = 3) were inoculated with H1N1pdm, H5N1, and H7N9/Ah at an MOI of 0.01. The infected organoids (cell lysate) (*Left*) and supernatants (*Center*) were harvested at the indicated times to detect the viral loads. Supernatant samples were used for viral titration (*Right*). Data are presented as mean ± SD. The experiment was performed three times independently. $^{**}P < 0.01$; $^{***}P < 0.005$.

AOs. Therefore, despite the discernible multilineage differentiation and the ability to support replication of IAVs, further improvements in morphology and differentiation appeared required.

PD of the AOs. To improve proximal differentiation (PD), we tried various protocols and variations thereof and settled on a medium described by Konishi et al. (18) for inducing ciliary differentiation in human PSC-derived airway epithelial spheroids. The ASC-derived organoids in the original AO medium gradually enlarged, while those in PD medium became more compact (Fig. 2*A*). After 16 d of culture, the organoids in AO medium grew approximately two times larger, while the organoids in PD medium remained basically unchanged in size (Fig. 2*B*). From day 7, the number of ciliated cells increased markedly in PD medium. At day 16, beating cilia were observed in a minority (<10%) of the organoids in AO medium, while abundant beating cilia were present in every PD organoid (Fig. 2*C* and Movies S2 and S3). The synchronously beating cilia drove the cell debris within the organoid lumens to swirl unidirectionally (Movie S3). The dramatically increased abundance of ciliated cells in the PD organoids was verified by immunofluorescence staining (Fig. 2*D*).

Consistently, the transcriptional levels of the ciliated cell markers FOXJ1 and SNTN were strongly up-regulated in the PD organoids compared with the organoids in AO medium. The expression levels of the basal cell markers P63 and CK5 and the goblet cell marker MUC5AC also increased, whereas the levels of club cell markers CC10 and SCGB3A2 were substantially

MICROBIOLOGY

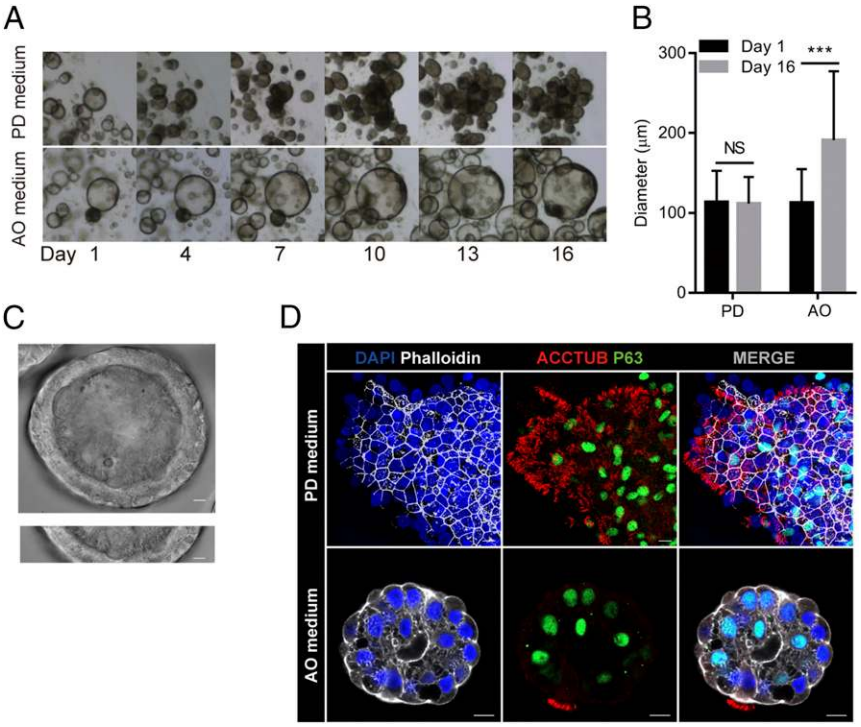

Fig. 2. PD of human AOs. (*A*) The AOs were cultured in PD medium or the original human AO medium in parallel for 16 d. Bright-field images of organoids at the indicated days are shown. (Magnification, 20×.) (*B*) Images of organoids cultured in PD medium and AO medium were used to measure the diameters of individual organoids (n = 300) using ImageJ. NS, not significant. ***$P < 0.005$. (*C*) Cilia in the PD AOs are captured by video. (Scale bar, 10 μm.) (*D*) Confocal images of $P63^+$ basal cells and $ACCTUB^+$ ciliated cells in the organoids cultured in PD and AO medium. (Scale bar, 10 μm.)

down-regulated in the PD organoids (Fig. 3*A*). Importantly, we observed globally elevated expression of serine proteases including TMPRSS2, TMPRSS4, TMPRSS11D (HAT), and matriptase, which are essential for the activation and propagation of human IAVs and low-pathogenic avian IAVs (8). We also performed flow cytometry analysis to measure the percentages of the four cell types in the organoids cultured in two distinct media at day 16. It was shown that the percentage of ciliated cells increased remarkably, by about threefold, after PD, to over 40% in the PD organoids, while the ciliated cells invariably constituted a minority of the cells in the organoids in AO medium (Fig. 3 *B* and *C*). Goblet cells also increased marginally, while club cells consistently decreased after PD (Fig. 3 *B* and *C*). Collectively, we successfully induced mucociliary differentiation and developed PD AOs which morphologically and functionally simulate human airway epithelium.

PD AOs Can Identify Human-Infective Virus. One of the most important and challenging issues for influenza research is to predict which animal or emerging influenza virus can infect humans. As mentioned above, the novel reassortant avian H7N9 viruses have caused continuing poultry-to-human transmission since 2013. In fact, other subtypes of avian IAVs, including H7N2, H9N2, and H9N9, have been cocirculating with the H7N9 viruses in domestic poultry. These viruses are highly similar in internal genes but differ in neuraminidase (NA) or HA and NA (19). However, very few human infections by H7N2, H9N2, and H9N9 virus have been reported in the same territory and time frame, although people were exposed equivalently to these viruses and the H7N9 viruses (20); these findings suggest that these viruses are less infective to humans than the H7N9 viruses.

We isolated, plaque-purified, and genotyped these cocirculating viruses. We chose to compare the infectivity of H7N2 with that of H7N9/Ah in the PD organoids as a proof of concept, to verify that the differentiated AOs can indeed simulate human airway epithelium in the context of influenza virus infection. Fig. 4 shows that viral loads in the cell lysate and medium of H7N9/Ah-infected organoids increased gradually after inoculation; the viral titer increased more than 3 $\log_{10}$ units within 24 h, indicating a robust viral replication. The addition of the serine protease inhibitor AEBSF significantly restricted the active replication of H7N9/Ah virus, highlighting the importance of elevated serine proteases for viral replication. In contrast, H7N2 propagated modestly, with viral titer 2–3 $\log_{10}$ units lower than H7N9/Ah. Thus, the distinct efficiencies of H7N9/Ah and H7N2 to infect and replicate in the PD AOs can recapitulate the infectivity of these viruses in humans.

Establishing a 2D Airway Monolayer from AOs to Assess the Infectivity of IAVs. A limitation of 3D organoids for studying microbial infections is the inaccessibility of the apical surface to pathogens, since most organoids are orientated inwards, while receptors for most respiratory viruses are distributed in the apical surface. For virus inoculation, organoids must be sheared to enable sufficient apical exposure to virus inoculum (21). As reported previously, primary bronchial epithelial cells cultured in Transwell inserts with the defined medium undergo mucociliary differentiation (22). This prompted us to transform 3D AOs into a 2D monolayer using Transwell culture. To this end, 3D AOs were enzymatically dissociated into a single-cell suspension, seeded in Transwell inserts, and then cultured in PD medium. The transepithelial electrical resistance (TEER) in the 2D monolayers stabilized in the second week after seeding (*SI Appendix*, Fig. S1). In addition, the dextran penetration assay performed at day 12 indicated that an intact epithelial barrier was formed across the 2D monolayers (*SI Appendix*, Fig. S1). The intense signal of ACCTUB indicated that the 2D monolayers developed appreciable PD (Fig. 5*A*). The productive infection of H7N9/Ah was clearly shown by the virus nucleoprotein-positive (NP^+) cells at 8 h post infection (hpi) in the 2D PD organoids (Fig. 5*A*).

To verify the ability of 2D PD organoids to assess the zoonotic potential of animal viruses and identify the human-infective virus, we compared the relative replication capacities of H7N9/Ah and H7N2 viruses and of another pair of viruses, the highly human-infective H1N1pdm and a swine H1N1 isolate (H1N1sw). The higher replicative capacity of H7N9/Ah over H7N2 virus was

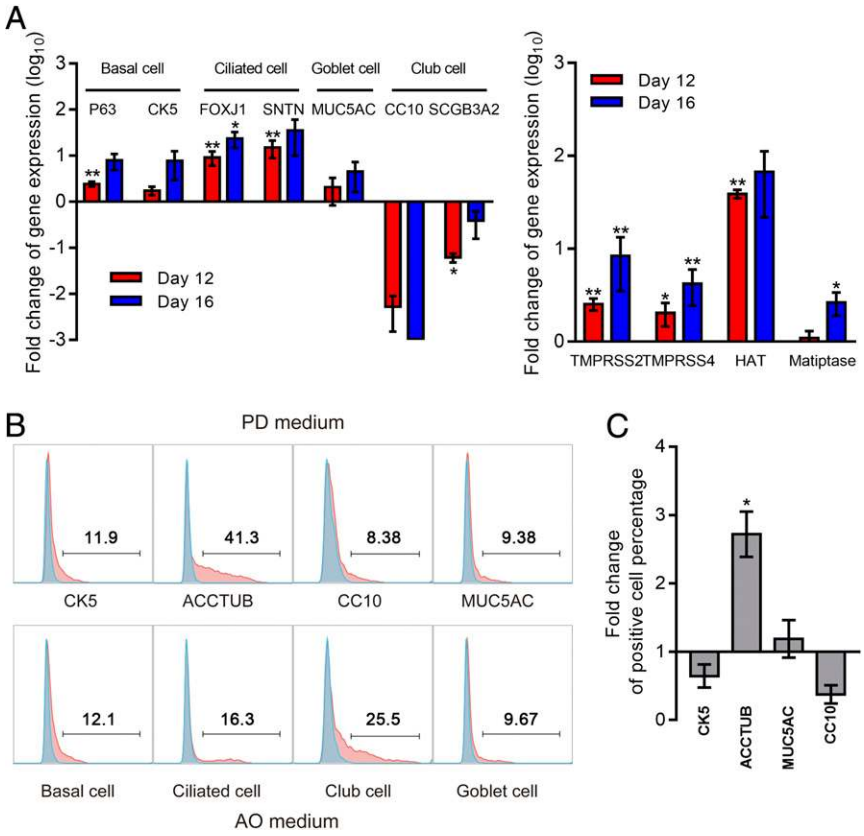

Fig. 3. Characterization of the differentiation status of AOs. (*A*) Fold changes in expression levels of cell-type markers (*Left*) and serine proteases (*Right*) in the organoids cultured in PD medium versus those cultured in AO medium at the indicated days. Data show the mean and SD of two lines of organoids. $*P < 0.05$; $**P < 0.01$. (*B*) The percentages of individual cell types in the organoids cultured in PD medium and AO medium. The representative histograms of one organoid line are shown. (*C*) Fold change in positive cell percentages in organoids cultured in PD medium versus those in AO medium. Data are presented as the mean and SD of four independent experiments. $*P < 0.05$.

more pronounced in the 2D PD organoids than in the 3D PD organoids; the viral titer of H7N9/Ah in the apical medium was 3–4 $\log_{10}$ units higher than that of the H7N2 virus (Fig. 5*B*). Consistently, H1N1pdm replicated dramatically, with a viral titer in the apical medium 1–2 $\log_{10}$ units higher than that of H1N1sw. Due to the epithelial barrier formed in the 2D monolayers and the preferential release of virus from the cell apical side, the viral titers in the basolateral medium were consistently lower than those in apical medium at the corresponding time points. Nevertheless, the differences in replicative capacity between H7N9/Ah versus H7N2 and H1N1pdm versus H1N1sw were even more prominent in basal medium than in apical medium at most time points.

Discussion

In this study, we describe the PD of human ASC-derived AO culture for investigating a major animal and human pathogen, influenza virus. In particular, our differentiation conditions increase the numbers of ciliated cells (Fig. 2), the major cell type in the human airway epithelium. The PD medium induces ciliated cell numbers to a nearly physiological level, with synchronously beating cilia readily discernible in every organoid (Movies S2 and S3). In addition, the expression levels of serine proteases (Fig. 3), known to be important for productive viral infection, were elevated after PD. Among the up-regulated HA-activating serine proteases, the dramatically increased expression of HAT in the differentiated AOs can very likely be attributed to the increased abundance of ciliated cells, since ciliated cells are the main source of HAT in the human respiratory tract (23). Thus, the differentiated AOs can simulate the human airway epithelium morphologically and functionally. As a further improvement, we developed 2D PD airway monolayers with an intact epithelial barrier to allow exclusively apical exposure to viruses (Fig. 5*A* and *SI Appendix*, Fig. S1), the natural mode of IAV infection in the human respiratory tract. We then utilized two pairs of viruses with known infectivity to demonstrate, as a proof of concept, that these organoids indeed show significantly higher susceptibility to the human-infective viruses than to the poorly human-infective viruses. These 3D and 2D differentiated AOs support the active replication of human-infective H7N9/Ah and H1N1pdm. In contrast, the H7N2 virus, which has been temporally and spatially cocirculating with H7N9 viruses in domestic poultry and contains internal genes similar to those in H7N9 viruses, replicated much less efficiently in both models. Similarly, the swine H1N1 isolate showed a substantially lower growth capacity than its counterpart, human-adapted H1N1pdm (Fig. 5*B*).

The avian IAV H7N2 subtype viruses have been circulating in the bird market from 1994–2006 and have caused poultry outbreaks in the United States. Sporadic human infections have been reported in the United States and Europe. Fortunately, all

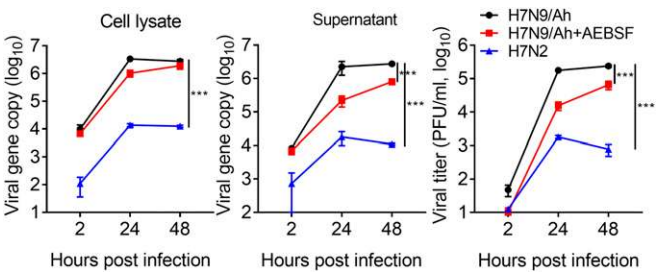

Fig. 4. Influenza virus infection in the 3D PD AOs. The 3D PD AOs ($n = 3$) were inoculated with H7N9/Ah and H7N2 virus at an MOI of 0.01. The infected organoids (cell lysate) and supernatants were harvested at the indicated times to detect the viral loads (*Left* and *Middle*). Supernatant samples were used for viral titration (*Right*). The experiment was performed three times independently. $***P < 0.005$.

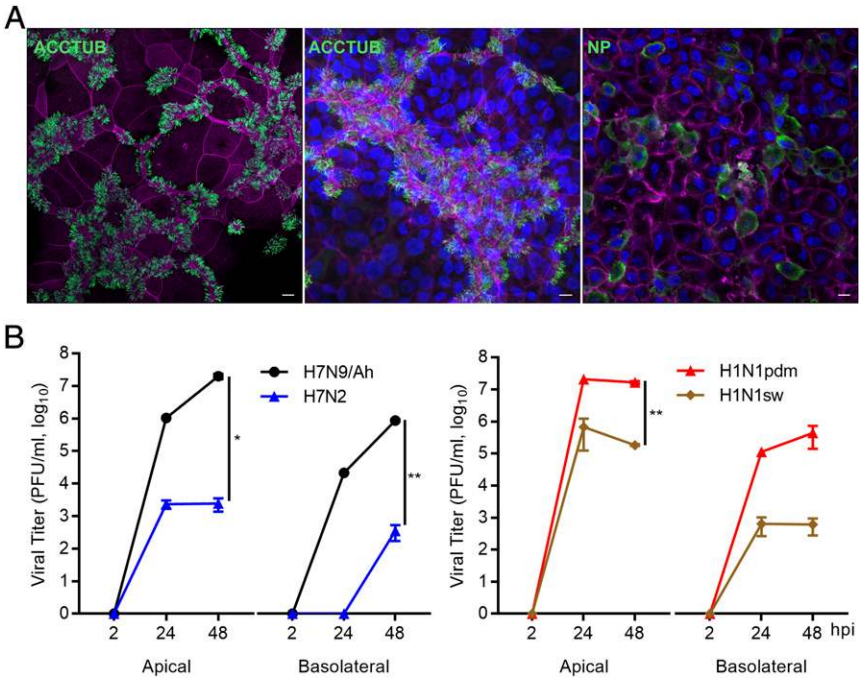

Fig. 5. Establishment of 2D differentiated AOs and replication capacity of influenza viruses. (*A*) Confocal images of the abundant ACCTUB$^+$ ciliated cells (*Left* and *Center*) taken in LSM 800 and 780 microscopes, respectively, and H7N9/Ah-infected (NP$^+$) cells (*Right*) in the 2D PD AOs. Nuclei and cellular actin filaments were counterstained with DAPI (blue) and Phalloidin-647 (purple). (Scale bar, 10 μm.) (*B*) The 2D PD AOs (n = 2) were inoculated with H7N9/Ah and H7N2 (*Left*) and H1N1pdm and H1N1sw (*Right*) at an MOI of 0.001. The cell-free media were harvested from the apical and basolateral chambers at the indicated times for viral titration. The experiment was performed three times independently.

reported cases of human infection experienced mild influenza-like symptoms (24). While pigs are considered the intermediate hosts for interspecies transmission of IAVs, swine influenza viruses lacking human adaptation markers rarely infect humans. Sporadic human infections documented in the literature or reported by public health officials are generally mild or subclinical (25). The ability of the PD AOs to differentiate avian H7 subtype virus and swine H1 subtype virus from the counterpart human-infective viruses suggests that these models could be used to assess the cross-species transmission potential of emerging influenza viruses in humans. In this study, only four strains of virus were assessed in the differentiated AOs as a proof of concept. More virus strains should be evaluated to further understand the strengths and limitations of this PD AO model.

In summary, we believe that these differentiated AOs significantly extend the current armamentaria of the influenza research toolbox. ASC-derived organoids, once established, can be expanded indefinitely while displaying remarkable phenotypic and genotype stability. They thus overcome the limitations in reproducibility and availability of the current in vitro model systems. AOs can be easily established from human bronchiolar lavage material, allowing interindividual comparisons; AOs can also be readily modified by lentiviruses and CRISPR technologies and can be single-cell cloned (14). In combination with the molecular toolbox of the influenza virologist, the human differentiated AO model system offers great opportunities for studying virus and host factors that define the characteristics of this major animal and human pathogen.

Materials and Methods

Establishing ASC-Derived Human AOs. The generation of four lines ASC-derived human AOs was based on the previous protocol (14) with a success rate of 100%. Briefly, with ethical approval by the Institutional Review Board of the University of Hong Kong/Hospital Authority Hong Kong West Cluster (UW 13-364) and informed consent of the patients, small pieces of normal lung tissue (~0.2–0.6 cm^2 in size) adjacent to the diseased tissues were obtained from patients who underwent resection. The tissues were minced and digested with 2 mg/mL collagenase (Sigma Aldrich) for 1–2 h at 37 °C, followed by shearing using a glass Pasteur pipette (Drummond) and straining over a 100-μm cell strainer (FALCON). The resultant single cells were embedded in 60% Matrigel (Growth Factor Reduced Basement Membrane Matrix; Corning) and were seeded in 24-well suspension culture plates (Greiner Bio-One). After solidification, Matrigel droplets were maintained with AO culture medium (*SI Appendix*, Table S1) at 37 °C in a humidified incubator with 5% CO_2. The organoids were passaged every 2–3 wk. The bright-field images of the organoids were acquired using a Nikon Eclipse TS100 Inverted Routine Microscope.

PD of Human AOs. The AOs were split and maintained in AO medium for 3–7 d. The culture medium in half of the organoids was changed to PD medium, PneumaCult-ALI medium (STEMCELL Technologies) supplemented with 10 μM DAPT (Tocris). The organoids were then cultured in AO or PD medium for 16 d. Bright-field images were taken every 3 d. Diameters of individual organoids were measured with ImageJ (NIH). The movies of organoids were acquired using a total internal reflection fluorescent (TIRF) microscope (Movie S1) and a Nikon Eclipse Ti2 Inverted Microscope System (Movies S2 and S3). At the indicated times, the organoids in the different media were harvested for detection of cellular gene expression or for flow cytometry analysis.

Establishing 2D Differentiated AOs with Transwell Culture. Transwell culture of AOs was performed as described elsewhere (24, 25) with modifications. Briefly, the organoids were dissociated into single-cell suspensions after digested with 10× TrypLE Select Enzyme (Invitrogen) for 1–5 min at 37 °C, sheared using a Pasteur pipette, and strained over a 40-μm filter. Approximately 3.5 × 10^5 cells were seeded into each Transwell insert (product no. 3494; Corning). The cells were cultured in AO medium at 37 °C in a humidified incubator with 5% CO_2 for 1–2 d. When cells reached >90% confluence, the AO medium was changed to PD medium in both the apical and basal chambers. The medium was changed every other day, and the cells were maintained for 14 d. TEER was measured every other day using a Millicell ERS-2 Volt-Ohm Meter (EMD Millipore). To assess the integrity of the 2D organoid monolayer as an epithelial barrier, at day 12 after seeding, FITC–dextran with an average molecular weight of 10,000 (Sigma Aldrich) was added to the medium in the upper chamber at a concentration of 1 mg/mL followed by incubation at 37 °C for 4 h. Subsequently, the culture media were harvested from the upper and bottom chambers to detect the fluorescence intensity using the Victor XIII Multilabel Reader (PerkinElmer).

Propagation of IAVs. IAVs A/Anhui/1/2013(H7N9) (H7N9/Ah) and A/Hong Kong/415742/2009(H1N1) (H1N1pdm) (26) and a swine H1N1 isolate, A/swine/Guangdong/07 (H1N1sw; GenBank accession no. MH293472) were propagated in MDCK cells. At 72 hpi, cell-free medium was harvested, aliquoted, and stored at −80 °C. Avian IAVs H7N2 (A/pigeon/Zhejiang/DTID-ZJU01/1-1/2013; GenBank accession no. MH186147) and A/Vietnam/1194/04 (H5N1) (27) were propagated in special pathogen-free embryonated chicken

eggs at 37 °C for 36 h. The eggs were chilled overnight at 4 °C; then the virus-containing allantoic fluid was harvested, aliquoted, and stored at −80 °C. Virus titer was determined by plaque assay.

IAV Infection in Human AOs. The 3D AOs were sheared mechanically to expose the apical surface to the virus inoculum. The sheared organoids were then incubated with viruses at a multiplicity of infection (MOI) of 0.01 for 2 h at 37 °C. After washing, the inoculated organoids were re-embedded in Matrigel and then were cultured in the PD medium. In the H7N9/Ah and H7N2 infection in the 3D PD organoids, one set of H7N9/Ah-inoculated organoids was treated with the serine protease inhibitor AEBSF (0.125 mM; Merck Millipore) during inoculation and after inoculation. At the indicated times, organoids, dissolved Matrigel, and culture medium were harvested for detection of viral load. The cell-free Matrigel and the culture medium from each droplet were pooled together as one sample, referred as the "supernatant." The supernatant samples were also used for viral titration. The 2D PD AOs were inoculated with the indicated viruses at an MOI of 0.001 from the apical side by adding the virus inoculum to the apical chamber followed by incubation for 2 h at 37 °C. At the indicated times, cell-free media were collected from the apical and basolateral chambers for viral titration. The membranes seeded with 2D organoids were incised from the Transwell inserts and fixed, and immunofluorescence staining was applied as described previously (13).

RNA Extraction and RT-qPCR. To evaluate the differentiation status of AOs cultured in PD medium versus those in AO medium, the organoids were harvested at the indicated times, and RNA was extracted using MiniBEST Universal RNA Extraction Kit (TaKaRa). To quantify virus replication, the organoids and supernatant samples were lysed for RNA extraction using the MiniBEST Universal RNA Extraction Kit and MiniBEST Viral RNA/DNA Extraction Kit (TaKaRa), respectively. cDNA was synthesized with the Transcriptor First Strand cDNA Synthesis Kit (Roche) with Oligo-dT primer. qPCR was performed with LightCycler 480 SYBR Green I Master Mix (Roche) using gene-specific primers (*SI Appendix*, Table S2) to detect cellular gene-expression level and viral gene copy number. The mRNA expression levels of cellular genes were normalized with that of GAPDH. Viral gene copy number was determined by absolute quantification using a plasmid expressing a conserved region of the IAV *M* gene.

Plaque Assay. A plaque assay was performed to determine titers of the virus stocks and supernatant samples as described elsewhere (26), with minor modifications. Briefly, MDCK cells were seeded in 12-well plates. Confluent monolayers were inoculated with 400 μL of 10-fold serial dilutions of samples and were incubated for 1 h at 37 °C. After the inoculum was removed, the monolayers were overlaid with 1% low melting point agarose (Invitrogen) supplemented with Eagle's minimal essential medium (MEM) and 1 μg/μL TPCK-treated trypsin and were further incubated for 2–3 d. The monolayers were fixed with 4% paraformaldehyde (PFA) and were stained with 1% crystal violet to visualize the plaque after the agarose plugs were removed. Virus titers were calculated as plaque-forming units per milliliter.

Immunofluorescence Staining. To identify the indicated cell types and the virus-infected cells, immunofluorescence staining was applied to the 3D and 2D AOs. Briefly, the organoids were fixed with 4% PFA, permeabilized with 0.1–5% Triton X-100, and blocked with Protein Block (Dako). Then the organoids were incubated with primary antibodies (*SI Appendix*, Table S3) diluted in Antibody Diluent buffer (Dako) overnight at 4 °C, followed by incubation with secondary antibodies (*SI Appendix*, Table S3) for 1–2 h at room temperature. Nuclei and actin filaments were counterstained with DAPI (Invitrogen) and Phalloidin-647 (Sigma Aldrich), respectively. The confocal images were acquired using a Carl Zeiss LSM 780 or 800 confocal microscope.

Flow Cytometry Analysis. To assess the percentages of four types of cells, the AOs were analyzed by flow cytometry. Briefly, the organoids were dissociated with 10 mM EDTA (Invitrogen) for 30–60 min at 37 °C, fixed with 4% PFA, and permeabilized with 0.1% Triton X-100. Subsequently, the cells were incubated with primary antibodies (*SI Appendix*, Table S3) for 1 h at 4 °C followed by staining with secondary antibodies. A BD FACSCanto II system was used to analyze the samples.

Statistical Analysis. Student's *t* test was used for data analysis. $P < 0.05$ was considered statistically significant. $^{*}P < 0.05$; $^{**}P < 0.01$. $^{***}P < 0.005$.

ACKNOWLEDGMENTS. We thank the Faculty Core Facility, Li Ka Shing Faculty of Medicine, University of Hong Kong, for assistance in confocal imaging and flow cytometry analysis. This work was supported in part by donations from the Shaw Foundation Hong Kong, Richard Yu and Carol Yu, Michael Seak-Kan Tong, the Respiratory Viral Research Foundation Limited, the Hui Ming, Hui Hoy and Chow Sin Lan Charity Fund Limited, and the Chan Yin Chuen Memorial Charitable Foundation; by Grant C7011-15R from the Collaborative Research Fund of the Research Grants Council; The Government of Hong Kong Special Administrative Region; the Collaborative Innovation Center for Diagnosis and Treatment of Infectious Diseases, Ministry of Education of China; and by Grant 2014ZX10004001004 from the National Project of Infectious Disease, Ministry of Science and Technology of China.

1. Klenk HD (2014) Influenza viruses en route from birds to man. *Cell Host Microbe* 15: 653–654.
2. To KK, Chan JF, Chen H, Li L, Yuen KY (2013) The emergence of influenza A H7N9 in human beings 16 years after influenza A H5N1: A tale of two cities. *Lancet Infect Dis* 13:809–821.
3. Chen Y, et al. (2013) Human infections with the emerging avian influenza A H7N9 virus from wet market poultry: Clinical analysis and characterisation of viral genome. *Lancet* 381:1916–1925.
4. World Health Organization (2017) Human infection with avian influenza A(H7N9) virus China. Available at www.who.int/csr/don/26-october-2017-ah7n9-china/en/WHO. Accessed May 30, 2018.
5. Dawood FS, et al.; Novel Swine-Origin Influenza A (H1N1) Virus Investigation Team (2009) Emergence of a novel swine-origin influenza A (H1N1) virus in humans. *N Engl J Med* 360:2605–2615.
6. Böttcher E, et al. (2006) Proteolytic activation of influenza viruses by serine proteases TMPRSS2 and HAT from human airway epithelium. *J Virol* 80:9896–9898.
7. Bosch FX, Garten W, Klenk HD, Rott R (1981) Proteolytic cleavage of influenza virus hemagglutinins: Primary structure of the connecting peptide between HA1 and HA2 determines proteolytic cleavability and pathogenicity of avian influenza viruses. *Virology* 113:725–735.
8. Böttcher-Friebertshäuser E, Klenk HD, Garten W (2013) Activation of influenza viruses by proteases from host cells and bacteria in the human airway epithelium. *Pathog Dis* 69:87–100.
9. Butler CR, et al. (2016) Rapid expansion of human epithelial stem cells suitable for airway tissue engineering. *Am J Respir Crit Care Med* 194:156–168.
10. Clevers H (2016) Modeling development and disease with organoids. *Cell* 165: 1586–1597.
11. Sato T, et al. (2011) Long-term expansion of epithelial organoids from human colon, adenoma, adenocarcinoma, and Barrett's epithelium. *Gastroenterology* 141:1762–1772.
12. Ettayebi K, et al. (2016) Replication of human noroviruses in stem cell-derived human enteroids. *Science* 353:1387–1393.
13. Zhou J, et al. (2017) Human intestinal tract serves as an alternative infection route for Middle East respiratory syndrome coronavirus. *Sci Adv* 3:eaao4966.
14. Sachs N, et al. (2018) Long-term expanding human airway organoids for disease modelling. *bioRxiv*, 10.1101/318444.
15. Chen YW, et al. (2017) A three-dimensional model of human lung development and disease from pluripotent stem cells. *Nat Cell Biol* 19:542–549.
16. Nikolić MZ, et al. (2017) Human embryonic lung epithelial tips are multipotent progenitors that can be expanded in vitro as long-term self-renewing organoids. *eLife* 6: e26575.
17. Yaghi A, Dolovich MB (2016) Airway epithelial cell cilia and obstructive lung disease. *Cells* 5:E40.
18. Konishi S, et al. (2016) Directed induction of functional multi-ciliated cells in proximal airway epithelial spheroids from human pluripotent stem cells. *Stem Cell Reports* 6: 18–25.
19. Han J, et al. (2014) Cocirculation of three hemagglutinin and two neuraminidase subtypes of avian influenza viruses in Huzhou, China, April 2013: Implication for the origin of the novel H7N9 virus. *J Virol* 88:6506–6511.
20. Yuan R, et al. (2017) Human infection with an avian influenza A/H9N2 virus in Guangdong in 2016. *J Infect* 74:422–425.
21. Drummond CG, et al. (2017) Enteroviruses infect human enteroids and induce antiviral signaling in a cell lineage-specific manner. *Proc Natl Acad Sci USA* 114: 1672–1677.
22. Matrosovich MN, Matrosovich TY, Gray T, Roberts NA, Klenk HD (2004) Human and avian influenza viruses target different cell types in cultures of human airway epithelium. *Proc Natl Acad Sci USA* 101:4620–4624.
23. Takahashi M, et al. (2001) Localization of human airway trypsin-like protease in the airway: An immunohistochemical study. *Histochem Cell Biol* 115:181–187.
24. Marinova-Petkova A, et al. (2017) Avian influenza A(H7N2) virus in human exposed to sick cats, New York, USA, 2016. *Emerg Infect Dis* 23.
25. Krueger WS, Gray GC (2013) Swine influenza virus infections in man. *Swine Influenza*, eds Richt JA, Webby RJ (Springer Berlin Heidelberg, Heidelberg), pp 201–225.
26. Zheng B, et al. (2010) D225G mutation in hemagglutinin of pandemic influenza H1N1 (2009) virus enhances virulence in mice. *Exp Biol Med (Maywood)* 235:981–988.
27. Zheng BJ, et al. (2008) Delayed antiviral plus immunomodulator treatment still reduces mortality in mice infected by high inoculum of influenza A/H5N1 virus. *Proc Natl Acad Sci USA* 105:8091–8096.